

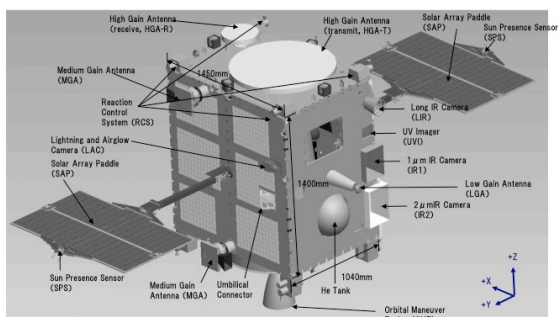
## Venus Orbit Insertion of Venus Climate Orbiter "AKATSUKI" in 2015

NAKAMURA, Masato<sup>1\*</sup> ; PLANET-C, Project team<sup>1</sup>

<sup>1</sup>Institute of Space and Astronautical Science

Venus Climate Orbiter AKATSUKI will be put into the Venus orbit in 2015. We will describe the detail of this challenge.

Keywords: Venus Atmosphere, Exploration



## Interannual Variability of Venus Albedo as Inferred from LASCO C3 Data

SATOH, Takehiko<sup>1\*</sup> ; ENOMOTO, Takayuki<sup>2</sup> ; SATO, Takao M.<sup>1</sup>

<sup>1</sup>JAXA, <sup>2</sup>SOKENDAI

Venus albedo in 4 bands (B, V, R, and IR) is measured in "superior conjunction" transits within LASCO C3 field of view. The data are available for 15 year period (1996-2011). The study is motivated by our recent finding of difference between 2 phase curves of Venus at small phase angles (Satoh et al., 2015; Mallama et al., 2006). The advantage of LASCO data is, needless to say, it is free of scattered light by the earth atmosphere to observe objects near the sun. With the field of view of LASCO C3 ( $30 R_{sun}$ ), up to 11 degrees phase angle of Venus can be studied.

Because Venus is too bright for nominal exposure time of LASCO (a few hundred seconds for faint coronae), the images of Venus is highly overexposed, resulting in saturation and blooming in the direction of charge transfer in CCD. We have developed a method to integrate such signals and evaluated its accuracy by measuring the brightnesses of stars (Aldebaran and Antares in IR). Measured star flux is found to be stable at the level of +/- 10 %, which is quite good as red-giants exhibit similar magnitude of pulsation.

In Venus data, we have found that brightness in IR seems to have changed between 2003 and 2005 transits. The data in 1996-2003 are systematically ~20 % brighter than the data in 2005-2011. It is noteworthy that Mallama et al.'s phase curves include the data from the former and Satoh et al.'s phase curves are in 2011 (the period of latter group). Details of data analysis and possible cause of such change will be discussed.

Keywords: Venus, Albedo, Interannual variation, SOHO, LASCO, C3

## The study of Venus transit for the extinction in the atmosphere of Venus and the plan for limb imaging by Akatsuki

KANAO, Miho<sup>1\*</sup> ; NAKAMURA, Masato<sup>1</sup> ; SHIMIZU, Toshifumi<sup>1</sup> ; OHTSUKI, Shoko<sup>2</sup> ; IMAMURA, Takeshi<sup>1</sup>

<sup>1</sup>JAXA/ISAS, <sup>2</sup>Senshu University

The study for the limb arc radiation from the solar photosphere observed during the transit of Venus will be reported following SGEPS meeting in 2014. The occulted flux observed by SOT is determined from some parameters; the solar flux, the refraction angle through the atmosphere of Venus, and the extinction by the atmosphere.

The solar flux is determined as the average un-occulted solar flux from the photosphere. The solid angle for the flux must change by the focusing effect and the spread due to the refraction angle gradient to the altitude. The refraction angle to the encountering solar radiation is calculated.

The flux in the atmosphere of Venus is decreased by the extinction due to the absorption and scattering by the molecular and the scattering by the cloud particles and the haze. The phase function of the Mie scattering for the cloud particles shows the strong forward peak. When the source function for the radiative-transfer equation is supposed to 0, the extinction due to the cloud particles could be derived from the Beer's law. Our goal is the accuracy on determining the number density of the cloud particles is better than 10 km and 1/cc in the atmosphere of Venus. The observation wavelength is 388.3 nm.

Akatsuki is planned to be inserted into Venus orbit in this year. We will be able to take images capturing the limb of Venus around the apoapsis. The plan to obtain the three-dimensional map of the cloud particles and the haze will be discussed.

Keywords: The atmosphere of Venus, Hinode, The solar occultation, Akatsuki, Aerosol

## Ground-based observation of 4.7um Venusian airglow

IWAGAMI, Naomoto<sup>1\*</sup> ; HOSOUCI, Mayu<sup>1</sup> ; KANO, Sakimi<sup>1</sup> ; HASHIMOTO, George<sup>2</sup>

<sup>1</sup>Univ of Tokyo, <sup>2</sup>Okayama Univ

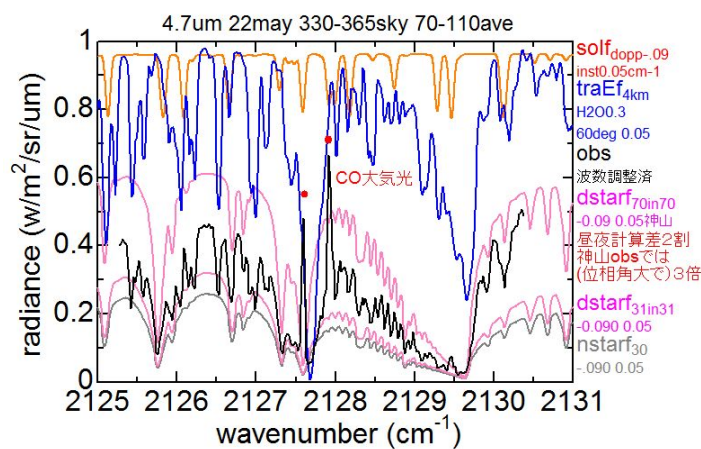
At first, the main part of the proposal on May 2014 to NASA/IRTF was 'To investigate the driving mechanism of the Super Rotation by comparing the waves at 60km by 1.7um spectroscopy and those at 70km by VEX/VMC'. Although agreement of simultaneous observation was there, it was canceled suddenly. Then we decided to get 70km data using 5um spectroscopy.

This is because cloud particles become black above 3um, and the height of tau=1 appears at 70km. This means the 5um observation will see waves at 70km. We selected 5.04um and 4.7um; the former is the region of least gas absorption and the latter is for comparison with Kouyama 4.7um data.

The 5.04um spectrum was successfully synthesized, but that at 4.7um was not with 2 emission lines appear at 2127.6 and 2127.9 cm<sup>-1</sup>. In the figure from top to bottom, solar(red), earth absorption(blue), Venus day(Kamiyama condition, pink), observed(black), Venus day(May condition, pink), Venus night(May condition, gray). A strong earth's CO absorption line is seen at 2127.6 cm<sup>-1</sup>. Those emission lines are seen even before sky subtraction on the Venus disk meaning them to be Venus origin.

However, no such pair of lines was found in HITRAN. I thought 'It may be a new finding?'. However, by searching old papers, it was found that the 4.7um Venus dayglow was observed 20 year ago. They are P4(1,0) and R2(2,1) lines, and the latter may be used to fined out CO distribution at the cloud top.

Keywords: venus, IR airglow, ground-based



## The cyclical nature of the propagation of planetary-scale UV feature changes within one Venus year

IMAI, Masataka<sup>1\*</sup> ; TAKAHASHI, Yukihiro<sup>1</sup> ; WATANABE, Shigeto<sup>1</sup> ; WATANABE, Makoto<sup>1</sup> ; KOUYAMA, Toru<sup>2</sup>

<sup>1</sup>Department of CosmoSciences, Graduate School of Science, Hokkaido University, <sup>2</sup>Information Technology Research Institute

Our ground-based Venus observations from mid-August 2013 to the end of June 2014 reveal that the periodical variation in the UV brightness changes within one Venus year and the traveling velocity is dominantly increased. Pioneer Venus spacecraft previously observed the periodical variation of UV brightness with the period 4-5 days, which caused by that the travel of planetary scale UV features [Del Genio and Rossow, 1982, 1990]. They suggested that the period of brightness variation corresponds to the propagation of planetary waves and it changes on a time scale of 5-10 years. Periodicity change can be argued as the vacillation of dynamical states and investigating the source of planetary waves is required to understand the Venus super-rotation.

Used instrument is an imager with 365 nm narrow-band filter installed on 1.6m Pirka telescope, which is operated by Hokkaido University, and we measured the UV brightness from equatorial to mid-latitudinal regions in both hemispheres. Our observations cover about one Venus year and have superiority for investigating the monthly change as compared to the Pioneer Venus observations.

We have two observational periods when the brightness has the prominent periodical variation. Latter season is considered to keep the periodicity for about two months. In August 2013, we detected about 5.2 days periodical brightness variation in equatorial and both northern and southern mid-latitudinal region. Bright and dark pattern had a prominent periodical and symmetric structure about the equator and we consider it is derived from a high contrast Y-feature such as previously observed by the Galileo spacecraft. On the other hand, after the mid-September 2013, there was no prominent and periodical brightness variation in the most of the observation time. In this season, the periodical and symmetric brightness structure has a cycle of being clear and unclear, and it suggests the Y-feature has a few weeks variation. From mid-September 2013 to the end of March 2014, periodical variation seems to be lost or one more accelerate and decelerate cycle should exist. In the last two months (from the beginning of May to the end of June 2014), however, it has 3.5 days period and perhaps last for about two months. Our study points out the possibility of the change of dynamical states occur in one Venus year.

Keywords: Venus, Pirka telescope, Super-rotation, UV feature

## Millimeter-Wave Band Monitoring Observations of the Terrestrial Planets in the Solar System with 10-m SPART Telescope

MAEZAWA, Hiroyuki<sup>1\*</sup>

<sup>1</sup>School of Science, Osaka Prefecture University

For understanding the influence of the activities of central stars on the middle and lower atmospheres of terrestrial planets in the solar system and of exoplanets, we have been performing monitoring observations of millimeter-waveband spectral lines of carbon monoxide ( $^{12}\text{CO}$ :  $J=1-0$  230.538 GHz,  $J=2-1$  115.2712018 GHz;  $^{13}\text{CO}$ :  $J=2-1$  230.3986765 GHz) in the middle atmospheres of Mars and Venus with a 10-m telescope, Solar Planetary Atmosphere Research Telescope (SPART), since it was launched in 2011. SPART employs highly sensitive 100- and 200-GHz double-band superconducting SIS heterodyne detectors and a 1-GHz-band digital fast-Fourier-transform spectrometer with a frequency resolution of 67 kHz. The heterodyne spectroscopy with high frequency resolution is a powerful tool to trace the weak and narrow spectral lines of minor constituents in the middle atmosphere of planets.

The results obtained with SPART suggest that the disk-averaged mixing ratio of carbon monoxide derived at an altitude of approximately 80 km in Venus has steadily decreased since 2012. The X- and M-class solar events that reached Venus also seem to have decreased from 2012 to 2014. To study the electron production rate induced by solar energetic particles incident at different altitudes of the planetary middle atmospheres, we also developed an analytical model, using which ionization losses are numerically calculated on the basis of the Bethe-Bloch formula. The ionization of carbon dioxide induced by solar-energetic-particle events is considered to increase the production rate of CO. With a basic model under conditions of typically great solar-proton events with incident-proton energies of less than 1 GeV, it was found that the ionization rate reaches its maximum at an altitude of 80-90 km in the Venusian atmosphere. These results suggest that the decrease in CO in the Venusian middle atmosphere may be deeply related to the solar activities.

In this conference, we will present these results and the status of the SPART project.

## Scientific capabilities and measurement sensitivities of the IR heterodyne spectroscopy

NAKAGAWA, Hiromu<sup>1</sup> ; SAGAWA, Hideo<sup>2</sup> ; AOKI, Shohei<sup>3</sup> ; KASABA, Yasumasa<sup>1</sup> ; MURATA, Isao<sup>1\*</sup> ;  
TAKAMI, Kosuke<sup>1</sup>

<sup>1</sup>Tohoku University, <sup>2</sup>Kyoto Sangyo University, <sup>3</sup>Istituto Nazionale di AstroFisica

Many molecules of atmospheric and astronomical interest exhibit rotational-vibrational spectra in the middle infrared (IR) regime. Fully resolved molecular features with high spectral resolution are possible retrieval of many physical parameters, such as density, velocity, pressure, excitation condition, temperature, and the vertical information from single line profile. In the mid-infrared wavelength region, the highest spectral resolution is provided by the IR heterodyne technique (Kostuik and Mumma, 1983). It is for the applications to astronomy and planetary atmospheric science in 7-13 micron wavelength at the spectral resolution of up to  $1E7-8$  (corresponds to 1-10m/s) with a very high sensitivity. Notable successes on Venus, Mars, Jupiter, Titan and Earth were given by NASA Goddard Space Flight Center, University of Cologne, and Tohoku University (Fukunishi et al. 1990; Taguchi et al., 1990; Goldstein et al., 1991; Kostuik, 1996; Kostuik et al., 2000; Sonnabend et al., 2012; Sornig et al., 2013) to date.

A new IR heterodyne instrument has been developed by Tohoku University for continuous monitoring of planetary atmospheres using dedicated ground-based telescopes (60cm and 1.8m) at Mt. Haleakala, Hawaii. Remarkable aspects of the instrument are (i) an excellent system noise temperature less than 3000K at 7-10 micron wavelength, (ii) a digital FFT spectrometer as a back-end with high resolution, stability, large dynamic range, flexibility, and the absence of optical or mechanical components, (iii) frequency tuneability over a wide range provided by the use of multi- room-temperature type quantum cascade laser as local oscillators to access various molecules.

Ultra-high resolution spectroscopic measurement ( $R=1E7$ ) is one of the most powerful tools to explore the planetary atmospheres with several key capabilities: (1) fully resolved molecular features to address the atmospheric temperature profiles, abundance profiles of the atmospheric compositions and their isotopes, (2) direct measurement of the mesospheric wind and temperature with high precision, (3) sensitive detection of minor trace gases, and (4) its small beam size capabilities to allow global mapping. The instrument is set on the Coude focus of the Tohoku 60cm-telescope at Mt. Haleakala in September 2014 to demonstrate the feasibility. The first Mars CO<sub>2</sub> non-LTE emission was successfully obtained in November 2014. Its continuous operation will be started from March 2015. Main targets in the verification process are Mars and Venus. Many interesting scientific issues have been targeted and more will be addressed in the future, i.e., planets, comets, the Earth, and the Sun. Extra solar objects like stars and stellar envelopes, proto-planetary disks are also possible targets of interest.

Here the scientific capabilities and measurement sensitivities of the instrument are specifically investigated by the radiative transfer models. We use the Advanced Model for Atmospheric TeraHertz Radiation Analysis and SimUlation (AMATERASU) that is being developed in the framework of NiCT. The model is based on the Microwave Observation and LInes Estimation and REtrieval (MOLIERE) (Baron et al., 2008; Mendrok et al., 2008). We simulated the temperature/wind retrievals from a single nadir observation of CO<sub>2</sub> absorption line at  $R12\ 970.5472\ \text{cm}^{-1}$ . Good temperature retrieval achieves in the rage from surface to 30km on Mars and from 65km to 95km on Venus with better than 10K precision and 10km vertical resolution. The local wind and temperature is directly derived at the middle atmosphere on Mars (75km) and Venus (110km) with 10m/s and 10K precision, respectively. These will enhance our understanding for the middle atmospheric dynamics and its fluctuations caused by the atmospheric waves from the lower atmosphere. Continuous monitoring of planetary atmospheres with its ultra-high resolution will open new insight for understanding the temporal/spatial variations in various time-scales.

Keywords: infrared, heterodyne, spectroscopy, Venus, Mars

## Time variation of wave structure in Jupiter's south polar region observed with ground-based telescope

GOUDA, Yuya<sup>1\*</sup> ; TAKAHASHI, Yukihiro<sup>1</sup> ; WATANABE, Makoto<sup>1</sup>

<sup>1</sup>Department of CosmoSciences, Graduate School of Science, Hokkaido University

A Rossby wave plays an important role in atmospheric phenomena on planets. For example, stratospheric sudden warming in the Earth is caused by a Rossby wave. The south polar wave at about  $67^{\circ}$  S in Jupiter is considered as one of signatures of Rossby wave. Previous observations, such as by Cassini ISS in 2000 or the Hubble Space Telescope (HST) from 1994 to 1999 [Barrado-Izagirre *et al.*, 2008], show that the polar region is covered by bright diffuse haze and its edge has a wavy structure spreading in longitudinal direction with wavenumber of 12 – 14 at  $67^{\circ}$  S, which travels westward with a phase velocity of 0 – 10 m/s in System III. These observations suggested that this wave structure is caused by a planetary Rossby wave. However, these observations had been carried out only every other year and the variance of short time scale (about month) is not clear.

We determine whether or not the wave observed at the edge of the stratospheric haze in south polar region is caused by Rossby wave. Using a methane absorption band filter at 889 nm installed at Multi-Spectral Imager (MSI) of the 1.6 m Pirka telescope, we investigated the meridional and vertical wavenumbers and phase velocity of the observed wave structure and zonal wind speed.

In this presentation, we introduce the results of analysis on the time variation of the wave structure in Jupiter's south polar region in 2011 to 2015 observed by the ground-based telescope. Each result is separated by two weeks to a few months in the periods that we can observe Jupiter. Our results show the wavy structure spreading in longitudinal direction at  $67^{\circ}$  S. However, our results are different from previous studies in two points. First, we cannot detect an apparent longitudinal motion of the wave structure in our observation periods. Second, there always exist darker areas by about two percent than surrounding longitude in the period of 2011 – 2014. In particular, longitude of about  $50^{\circ}$  and  $130^{\circ}$  in System III are always dark. These dark regions at 889 nm suggest that the cloud top altitude at  $67^{\circ}$  S is lower than pressure altitude of 360 mbar. We think there are another atmospheric structures, such as a local eddy or cloud convection, in Jupiter's south polar region other than those caused by a Rossby wave at  $67^{\circ}$  S. Our results may suggest that a combination of a planetary Rossby wave and local structure that is less than longitudinal width of  $15^{\circ}$  exists at about  $67^{\circ}$  S.

Keywords: Jupiter, haze, Rossby wave, polar area, ground-based telescope



## Mechanism for the formation of equatorial superrotation in forced shallow-water turbulence with Newtonian cooling

SAITO, Izumi<sup>1\*</sup> ; ISHIOKA, Keiichi<sup>1</sup>

<sup>1</sup>Graduate School of Science, Kyoto University

The zonally banded patterns and latitudinally alternating zonal jets are striking features of the atmospheres of Jupiter and Saturn. To explain the origin of these zonal structures, a series of studies considers large-scale motions within a shallow surface layer of a planetary atmosphere. One of the models for this "shallow layer" theory is forced shallow-water turbulence on a rotating sphere. This model can reproduce zonal structures and also other features observed in Jupiter and Saturn, such as vortical motions predominating in the polar region and zonal jets having larger amplitudes near the equator (Scott and Polvani, 2007). However, a problem of this model was that it cannot produce a robust equatorial superrotation, as observed in Jupiter and Saturn. This problem was overcome by Scott and Polvani (2008). They revealed that forced shallow-water turbulence can produce robust strong equatorial superrotation, if Newtonian cooling is adopted as the dissipation process instead of Rayleigh friction.

The purpose of the present study is to elucidate the mechanism of the robust formation of equatorial superrotation reported by Scott and Polvani (2008). It is shown that the Newtonian cooling term distorts the structure of the Hough modes. This distortion can be visualized as either the westward or eastward tilting of the equiphase line with increasing the absolute value of latitude; the structural change of the Hough modes leads to the acceleration of the zonal-mean flow. A statistical analysis based on a weak-nonlinear theory predicts that stochastically excited Hough modes generate a prograde equatorial jet, the profile of which is quantitatively consistent with that of the ensemble-averaged zonal-mean flow obtained in nonlinear time-evolutions. The predicted prograde equatorial jet originates mainly from the acceleration produced by Rossby modes, the equiphase line of which is tilted westward by the Newtonian cooling term.

(This work was recently published as Saito and Ishioka (2015))

### References:

Scott, R. K. and L. M. Polvani, 2007: Forced-dissipative shallow-water turbulence on the sphere and the atmospheric circulation of the giant planets. *J. Atmos. Sci.*, 64, 3158-3176.

Scott, R. K. and L. M. Polvani, 2008: Equatorial superrotation in shallow atmospheres. *Geophys. Res. Lett.*, 35, L24202.

Saito, I. and K. Ishioka, 2015: Mechanism for the formation of equatorial superrotation in forced shallow-water turbulence with Newtonian cooling. *J. Atmos. Sci.*, in press, now available in Early Online Release form.

Keywords: Jupiter, zonal pattern, forced shallow-water turbulence, equatorial superrotation, Newtonian cooling, Hough mode

## Disappearance of surface banded structure produced by thermal convection in rapidly rotating thin spherical shells

SASAKI, Youhei<sup>1\*</sup>; TAKEHIRO, Shin-ichi<sup>2</sup>; ISHIOKA, Keiichi<sup>3</sup>; NAKAJIMA, Kensuke<sup>4</sup>; HAYASHI, Yoshi-yuki<sup>5</sup>

<sup>1</sup>Department of Mathematics, Kyoto University, <sup>2</sup>Research Institute for Mathematical Sciences, Kyoto University, <sup>3</sup>Department of Earth and Planetary Sciences, Kyoto University, <sup>4</sup>Department of Earth and Planetary Sciences, Kyushu University, <sup>5</sup>Department of Earth and Planetary Sciences, Kobe University

Surface flows of Jupiter and Saturn are characterized by the broad prograde zonal jets around the equator and the narrow alternating zonal jets in mid- and high-latitudes. It is not yet clear whether those surface jets are the result of fluid motions in the "shallow" weather layer, or they are produced by convective motions in the "deep" region. "Shallow" models consider atmospheric motions driven by the solar differential heating and the intrinsic heat flow from the deeper region under the assumption of hydrostatic balance in the vertical direction as a result of the thin atmospheric layer compared with the radius of the planet. These models can produce narrow alternating jets in mid- and high-latitudes, while the equatorial jets are not necessarily prograde. On the other hand, "deep" models, which describe thermal convection in rapidly rotating spherical shells whose thickness is comparable to the radius of the planet, can produce equatorial prograde flows easily, while it seems to be difficult to generate alternating jets in mid- and high-latitudes.

Heimpel and Aurnou (2007)[1](hereafter, HA2007) proposed thin spherical shell models and show that the equatorial prograde zonal jets and alternating zonal jets in mid- and high-latitudes can be produced simultaneously when the Rayleigh number is sufficiently large and convection becomes active even inside the tangent cylinder. However, they assume eight-fold symmetry in the longitudinal direction and calculate fluid motion only in the one-eighth sector of the whole spherical shell. Such artificial limitation of the computational domain may influence on the structure of the global flow field. For example, zonal flows may not develop efficiently due to the sufficient upward cascade of two-dimensional turbulence, or stability of mean zonal flows may change with the domain size in the longitudinal direction. Further, since time integration of their numerical experiment is so short as 1600 rotation period (0.024 viscous diffusion time), their result may not reach statistically steady state. Therefore, in the present study, we perform long time numerical experiment of thermal convection in the whole thin spherical shell domain, where the experimental setup is same as that of HA2007.

We consider Boussinesq fluid in a spherical shell rotating with constant angular velocity. The non-dimensionalized governing equations consist of equations of continuity, motion, and temperature. The non-dimensional parameters appearing in the governing equations, the Prandtl number, the Ekman number, the modified Rayleigh number, and the radius ratio, are fixed to 0.1,  $3 \times 10^{-6}$ , 0.05, and 0.85, respectively. The initial condition of the velocity field is state of rest and that of the temperature field is conductive state with random temperature perturbations. After time integration for 7500 rotation period, An equatorial prograde surface zonal jet and alternating banded zonal jets emerge, which seem to be consistent with the result of HA2007. However, extending time integration further, mid- and high- latitudinal regions are entirely accelerated eastward, zonal banded structures disappear, and finally one broad eastward zonal jet appears in mid- and high- latitudes of each hemisphere around 12800 rotation period. Formation of these broad zonal jets is attributed to the angular momentum transport in the radially outward direction by topographic Rossby waves, which are excited by thermal convection inside the tangent cylinder. Note that further time integration is necessary to obtain statistically steady state since kinetic energy still increases in the final state of the present calculation.

Acknowledgement : Numerical computations were carried out on the Earth Simulator (ES2) at the Japan Agency for Marine Earth Science and Technology.

Reference : [1] Heimpel, M., Aurnou, J. (2007) *Icarus*, 187, 540–557.,

Keywords: atmospheres of the gas giant planets, banded structure, equatorial prograde jet, Rossby waves, Jupiter, Saturn

## Recent study of atmosphere change and proposed global water system on Venus and Mars

MIURA, Yasunori<sup>1\*</sup>

<sup>1</sup>Visiting Univ.(In & Out)

Introduction: Air and sea water of the Earth-type planets are applied from detailed database of global Earth planet, because huge database of water planet Earth which has been accumulated precisely by our human activity on global Earth is considered to be applied easily and precisely [1].

Characteristics of atmosphere formation: Global atmospheric gas of planets should be continued to be erupted from the interior of the planets with the gravity effect. Venus and Mars with volcanoes along the equators followed the planetary rotations have been released volatile molecules of carbon dioxides previously or now [1].

Characteristics of global water system: The presence of sea-water of Earth planet has been applied for the evidence of past global sea water because of volatile elements in the interior deposits.

However, the phase diagram of the fluid (water and carbon dioxide) suggests that liquid can be stable by sandwiched with solid and air phase [2, 3]. Therefore, global seawater system can be formed basically only for global air system of any planets (Venus and Mars), it is difficult problem of local fluid ions or molecules enough for global water system.

Challenge for changes in atmospheric composition: Primordial planet's atmosphere shows composition with carbon dioxide gas, where it's significant challenge of changed atmospheric composition for future habitable planet. Cold carbon dioxides on Martian air for melting and solidification are generally possible realistically. However hot carbon dioxides (on Venus) are generally difficult to be changed locally and globally. It might be possible to apply present artificial method to change hot gas solidified [4] on the surface (not underground interior) for global system finally.

The possible formation of water system: Volatile systems of air and water separated from solid rocks produce planets of higher density as in Earth and Venus. Therefore there are two dynamic methods to form water system on Venus and Mars of 1) step-by-step method, and 2) rapid evaporation and cooling method. It would be effective proposed methods to form global water system (Venus and Mars) by natural celestial collisions and artificial methods of present science and technology finally [4].

### Summary:

- 1) Formation of air and water systems for waterless Venus and Mars might be possible by experimental study based on new proposed research.
- 2) Air systems of Venus and Mars are considered to be internal volatile molecules emitted mainly by the planetary rotations.
- 3) Larger air-planets of Venus and Mars have environments for possible formation of water planets experimentally and naturally.
- 4) Global changes of cold air (Mars) and hot air (Venus) are possible based on effective scientific processes.
- 5) Global sea-water system for Venus and Mars by celestial activity and artificial methods is considered to be effective proposed methods.

### References:

- [1] Miura Y.(2011):International Venus Workshop(VEXAG)Meeting #9 (Virginia). #1, #2.
- [2] Miura Y. et. al. (1996) Antarctic Meteorites XX1(Tokyo), 107-110.
- [3] Miura Y. (2015): LPSC2016 (LPI), #1811, 1666.
- [4] Miura Y. (2009): Patent application.

Keywords: Venus, Mars, Air system, Sea water system, Compositional change, Hot carbon dioxides

## An MHD simulation study of magnetic reconnection in the dayside Venusian ionosphere

SAKAMOTO, Hitoshi<sup>1\*</sup> ; TERADA, Naoki<sup>1</sup> ; KASABA, Yasumasa<sup>1</sup>

<sup>1</sup>Graduate School of Science, Tohoku University

Venus and Mars have no significant global intrinsic magnetic field. However, it is considered that magnetic reconnection can occur in their ionospheres and magnetotails through the direct interaction with the solar wind. The occurrence frequency distribution of magnetic reconnection at the 400km altitude of Mars has been obtained from magnetic field and electron observations by Mars Global Surveyor [Halekas et al., 2009], but the occurrence frequency at other altitudes is yet to be obtained because of the limitation of its trajectory. In addition, the role of magnetic reconnection in determining the structure and dynamics of the ionospheres of unmagnetized planets has been unclear because there is no observation that constrains the relation among them. Not only observational studies but also theoretical studies have been needed for further understanding magnetic reconnection around unmagnetized planets, and we have studied magnetic reconnection caused by the rotation of interplanetary magnetic field (IMF) in their dayside ionospheres, using a two-dimensional multi-species magnetohydrodynamic (MHD) simulation.

We would infer that magnetic reconnection has a possible relation to some unexplained phenomena observed around the ionospheres of Mars and Venus, considering the dependences of their occurrence rate and spatial distribution on the rotation of IMF. One example is the ejection of plasma 'clouds' from their ionospheres [Brace et al., 1981; Crider et al., 2004]. The occurrence rate of this phenomenon is relatively high when the direction of IMF changes [Ong et al., 1991], and plasma 'clouds' can be ejected by magnetic reconnection caused by the IMF rotation. Another example is the existence of small magnetic rope-like structures called 'flux ropes' [Russell and Elphic, 1979; Cloutier et al., 1999]. When the solar wind dynamic pressure is low, 'flux ropes' are most often observed in the lower ionosphere [Elphic et al., 1983]. So far some models to generate the 'flux ropes' in the ionospheres have been proposed, e.g., Kelvin-Helmholtz instability at the ionopause [Wolff et al., 1980] and nonlinear effects in the lower ionosphere [Kleorin et al., 1994], and Dreher et al. [1995] suggested that magnetic reconnection due to the IMF rotation generates 'flux ropes' using a numerical simulation.

In this presentation, we will show the time evolution of magnetic reconnection in the dayside Venusian ionosphere and the structure of plasmoids obtained from the two-dimensional multi-species MHD simulation. We will present, in particular, the altitudes where magnetic reconnection effectively develops, the time scale of the development of magnetic reconnection, and the spatial scale of plasmoids generated by the reconnection. Our simulation result shows that multiple magnetic reconnections occur in the current sheet and plasmoids are generated above 240 km altitude, where the Lundquist number is more than  $10^6$ . It has been found that the inflow condition of the current sheet and the growth time of the fast resistive magnetic reconnection [Loureiro et al., 2007] are important factors in determining the altitudes where reconnection effectively develops. Plasma flows into the current sheet from the both side of it above a certain altitude, and reconnection is likely to occur under this inflow condition. However, the intrinsic downward flow in the Venusian lower ionosphere inhibits plasma from flowing into the sheet, which diminishes the reconnection rate below a certain altitude. In addition, we find that the growth time at the lower regions where the fast resistive reconnection does not occur is comparable to or shorter than the time scale of the transportation of magnetic field. We will examine whether the magnetic reconnection caused by the rotation of IMF generates the ejection of plasma 'clouds' and the 'flux ropes'.

Keywords: Venus, ionosphere, reconnection

## UV Space Telescope for extrasolar planetary systems

KAMEDA, Shingo<sup>1\*</sup> ; IKEZAWA, Shota<sup>1</sup> ; MURAKAMI, Go<sup>2</sup> ; NARITA, Norio<sup>3</sup> ; IKOMA, Masahiro<sup>4</sup> ;  
SEKINE, Yasuhito<sup>4</sup> ; YOSHIKAWA, Ichiro<sup>4</sup> ; SUGITA, Seiji<sup>4</sup>

<sup>1</sup>Rikkyo University, <sup>2</sup>JAXA, <sup>3</sup>NAOJ, <sup>4</sup>The University of Tokyo

Many observations have been performed for exoplanets since the first discovery in 1995. The number of detected exoplanets is more than 1800. Some of them orbit around a star with an orbital radius shorter than that of Mercury, which suggests that the high-intensity UV irradiation causes large amount of atmospheric loss.

Many exoplanets were discovered by observing transits. Exoplanetary atmospheric atoms and molecules absorb stellar photons, which causes wavelength-dependent transit depth, though transit depth of an exoplanet without any atmosphere is not wavelength-dependent. Therefore, we can know atmospheric composition from the result of spectroscopic observation of exoplanet transit.

The radius of the exoplanet HD209458b is approximately 1.4 R<sub>J</sub> and its semi-major axis is only 0.047 AU. It is called Hot Jupiter. Sodium, hydrogen, magnesium, and H<sub>2</sub>O have been detected in its atmosphere. Hydrogen was detected using the Hubble Space Telescope and the result shows the optically thick hydrogen atmosphere extends to three times farther than its radius. This also suggests that very large amount of atmospheric loss occurs in the exoplanetary system, which is not in the solar system.

NASA and ESA have already launched and are planning to launch space telescopes dedicated for exoplanets, however, their spectral range is limited to visible and infrared. Though the Hubble Space Telescope is the only telescope for UV range, the operation will be stopped in the near future because of its aging. In this presentation, we introduce our plan for a small UV space telescope project.

Keywords: exoplanet, ultraviolet, space telescope

## Long-term temporal variation of Mercury's sodium exosphere

YASUDA, Tatsuya<sup>1\*</sup> ; KAMEDA, Shingo<sup>1</sup> ; KAGITANI, Masato<sup>2</sup> ; YONEDA, Mizuki<sup>2</sup> ; OKANO, Shoichi<sup>2</sup>

<sup>1</sup>Rikkyo University, <sup>2</sup>Tohoku University

Mercury has a very thin atmosphere. It has been observed by space probes Mariner 10 and MESSENGER, and by ground-based observations, to have hydrogen (H), helium (He), oxygen (O), sodium (Na), potassium (K), and calcium (Ca) atoms in its atmosphere. These atoms emit light, with resonance scattering caused by energy from sunlight. Because of its high intensity, the emission of sodium atoms is well suited for studies by ground-based observations. The source processes of Mercury's exosphere are considered to be solar-photon-stimulated desorption, "sputtering" by impacting solar wind particles crashing into Mercury's surface and releasing atoms, and interplanetary dust vaporization. Combination of these three processes is considered to arise, but the primary process among them is unknown as yet.

At the Haleakala Observatory in Hawaii we have observed daily variation of Mercury's sodium exosphere. The observations were performed using a 40 cm Schmidt-Cassegrain telescope, a high-dispersion spectrograph, and a charge coupled device (CCD) camera. During observation seasons, elongation between Mercury and sun is more than 15 degrees, and observation time varies from 30 min to 1 h before sunrise or after sunset. The exospheric emission observed from the ground is part rather than entire dayside. The ratio of the observed emission varies by phase angle. Thus, we estimated the number of sodium atoms above entire dayside, using the exospheric model and assuming constant exospheric temperature.

Interplanetary dust is known to be distributed densely to the plane called dust symmetry plane, but the detailed distribution in the vicinity of Mercury is not known. To verify the contribution of interplanetary dust impact to exospheric yield, model parameters which maximize correlation coefficient was derived, based on simplified dust distribution model by Kelsall et al. [1998]. Inclination and ascending node in this model are based on observation of zodiacal light by Helios 1, 2. This model fitting shows that the number of sodium atoms correlates highly with interplanetary dust density. The correlation coefficient is 0.856. This result indicates that interplanetary dust vaporization may contribute significantly to the exospheric yield.

The impact of interplanetary dust mixes grains at the surface and replaces depleted grains with fresh grains. This is known as gardening effect. In addition, interplanetary dust contains sodium and therefore supplies sodium atoms to the surface, which increases the source rate by other processes.

Keywords: Mercury, exosphere

## Heavy ion kinetics in Mercury magnetosphere with offset dipole

YAGI, Manabu<sup>1\*</sup> ; SEKI, Kanako<sup>2</sup> ; MATSUMOTO, Yosuke<sup>3</sup> ; DELCOURT, Dominique<sup>4</sup> ; LEBLANC, Francois<sup>4</sup>

<sup>1</sup>PPARC, Tohoku University, <sup>2</sup>STEL, Nagoya University, <sup>3</sup>Chiba University, <sup>4</sup>CNRS

Based on observations by MESSENGER, Mercury magnetosphere is thought to be a miniature of the Earth magnetosphere. These two magnetospheres have several characteristics in common, however, some critical differences are also evident. First, there is no atmospheric layer, but only tenuous exosphere. Second, the kinetic effects of heavy ions might not be negligible because Mercury magnetosphere is relatively small compared to the large Larmor radii. Trajectory tracings is one of the dominant methods to estimate the kinetic effect of heavy ions which originate the exosphere, though the results of the simulation are quite sensitive to the electric and magnetic field. Therefore, it is important to provide a realistic field model in the trajectory tracings. In order to construct a large scale structure, we developed a MHD simulation code, and adopted to the global simulation of Mercury magnetosphere. We performed four solar wind conditions of the northward IMF, and the results showed that the global configurations such as the location of magnetopause depend heavily on the dynamic pressure, while the solar wind electric field contributes little to the magnetospheric configuration. On the other hand, the results of statistical trajectory tracings of exospheric sodium ions depend not only on the dynamic pressure but also on the solar wind electric field. In the results, we identified two efficient acceleration processes and formation of the sodium ring which is formed by the accelerated ions drifting around the planet by magnetic gradient of the dipole field. When the solar wind dynamic pressure is low, acceleration by magnetospheric convection is efficient in the vicinity of Mercury. When the dynamic pressure is high, entry of the accelerated ions picked-up in the magnetosheath into the magnetosphere becomes dominant. The entry point of sodium ions changes due to the variation of the solar wind electric field, which causes a difference in the sodium ring's shape for the same solar wind dynamic pressure cases. Recent observation by MESSENGER revealed the weaker dipole field of Mercury than the past estimation based on Mariner 10 as well as large offset of dipole which could change the global configuration of Mercury magnetosphere and behavior of sodium ions. In the presentation, we will also discuss the ongoing simulation including the above configuration of intrinsic magnetic field of Mercury especially focus on how will this affect the distribution of sodium ions and its acceleration mechanisms.

Keywords: Mercury magnetosphere, MHD, test particle, sodium ion, offset dipole

## Formation of vortex configuration in the high resolution simulation of Kronian magnetosphere

FUKAZAWA, Keiichiro<sup>1\*</sup>

<sup>1</sup>Academic Center for Computing and Media Studies, Kyoto University

In a series of our simulation studies we have found turbulent convection and vortices formed at Saturn's dawn and dusk magnetopause in simulations when IMF was northward. We interpreted these vortices as resulting from the Kelvin Helmholtz (K-H) instability. The resolution of simulation is important parameter for formations of vortex and turbulent convection to catch the small configuration of convection which can be a trigger of vortex. Recently we can perform the higher resolution simulation (0.06Rs) of our previous simulation (0.3 or 0.1Rs) thanks to the evolution of computer technologies. In this study we run the simulation of Kronian magnetosphere with various IMF conditions to see the configuration of vortex and magnetospheric convection.

As the results of simulations the vortex does not appear in the no IMF and weak northward IMF condition. Adding the mean magnitude of northward IMF, we obtained the vortex along the magnetopause in the dawn and dusk. The difference of overall configuration between the weak and normal northward IMF is formation of vortex and other configurations very resemble. From these results we will discuss the formation condition of vortex in the Kronian magnetosphere and their configurations.

Keywords: Kronian magnetosphere, numerical simulation



## Fine structure of Jupiter's decametric modulation lanes observed by LWA1

IMAI, Kazumasa<sup>1\*</sup> ; SHIMANOUCI, Yoshiaki<sup>1</sup> ; IMAI, Masafumi<sup>2</sup> ; CLARKE, Tracy<sup>3</sup> ; HIGGINS, Charles A.<sup>4</sup>

<sup>1</sup>Kochi National College of Technology, <sup>2</sup>Kyoto University, <sup>3</sup>Naval Research Laboratory, <sup>4</sup>Middle Tennessee State University

The Long Wavelength Array (LWA) is a low-frequency radio telescope designed to produce high-sensitivity, high-resolution images in the frequency range of 10-88 MHz. The Long Wavelength Array Station 1 (LWA1) is the first LWA station completed in April 2011, and is located near the VLA site in New Mexico, USA. LWA1 consists of a 256 element array, operating as a single-station telescope.

The sensitivity of the LWA1 combined with the low radio frequency interference environment allow us to observe the fine structure of Jupiter's decametric modulation lanes. At frequencies in the vicinity of 22 MHz, most modulation lane patterns have frequency-time slopes between +100 and +180 kHz/sec for Io-B storms and between -90 and -200 kHz/sec for Io-A and Io-C storms. The lanes generally display a strong periodicity in time, with periods ranging from about 1 to 5 sec and an average of about 2 sec.

We refer to the modulation lanes possessing frequency-time slopes and periodicity within the above ranges as the major component. There is a minor modulation lane component, representing a considerably smaller fraction of the total number observed, for which the frequency-time slopes are of opposite sign than for the major component or are of the same sign but of smaller absolute value. For these cases the lanes are usually broader and their separations in time are longer.

There are significant differences of characteristics between the major and the minor components of modulation lanes. Minor component lanes are apparently of somewhat different origin from major component lanes. We show the fine structure of the major and minor modulation lanes observed by the LWA1. The origin of minor modulation lanes is discussed.

Keywords: Jupiter radio, decametric wave, modulation lane, fine structure

## Feasibility of the exploration of the subsurface ocean of Jupiter's icy moon by Jovian decametric radiation spectra

KUMAMOTO, Atsushi<sup>1\*</sup> ; KASABA, Yasumasa<sup>1</sup> ; MISAWA, Hiroaki<sup>1</sup> ; TSUCHIYA, Fuminori<sup>1</sup>

<sup>1</sup>Tohoku University

Subsurface liquid ocean of the Jupiter's icy moons, which is suggested by several studies, is one of the most important targets in the Jovian exploration missions. We propose a new method for determination of the depth of the boundary between the icy crust and liquid ocean below the icy crust by using interference patterns found in the spectrogram of the Jovian decametric radio emissions (DAM). If we can operate an wave receiver onboard the icy moon orbiter, we can obtain spectrograms of the DAM propagated from Jupiter. Because the emissions directly from Jupiter can be interfered with the emissions reflected at the icy moon's surface and subsurface boundaries, we will find interference patterns in the measured spectrograms. In case of the Moon, the lunar orbiter SELENE detected the interference patters in the spectrograms of auroral kilometric radiation (AKR) [Ono et al., 2010]. Because the interference occurs between AKR directly from the earth and AKR reflected at the lunar surface, the amplitude of the interference patterns are almost constant. In case of Jupiter's icy moons, DAM directly from Jupiter, DAM reflected at the icy crust surface, and DAM reflected at the boundary between icy crust and liquid ocean are interfered with each other. Due to slight phase difference between DAM emissions reflected at the surface and subsurface boundaries, the amplitude of the interference patterns will be modulated. The depth of the liquid ocean can be determined the frequency width of the modulation. Assuming that the frequency of DAM is ~25 MHz, the permittivity of the icy crust is 3, permittivity of the liquid ocean is 87, loss rate in the icy crust is 1 dB/km, and the depth of the ocean is 5 or 10 km, spacecraft and receiver's specifications needed for measurement of the interference patterns in the spectrogram are as follows: (1) Spacecraft height below 200 km, (2) Receiver bandwidth of <1 kHz, and (3) Receiver level resolution of <5 dB. In addition, the following two issues have to be considered in actual application of this method: (a) DAM itself has band structures in the spectrogram due to anisotropy of the emission at the source. (b) The roughness of the surface and subsurface boundaries have to be within the wavelength (~10 m) in order that the interference occurs.

Keywords: Jupiter's icy moon, Subsurface ocean, Jovian decametric radiation, Interference

## The Circumpolar Stratospheric Telescope FUJIN for Observations of Planets

MAEDA, Atsunori<sup>1\*</sup>; TAGUCHI, Makoto<sup>2</sup>; SHOJI, Yasuhiro<sup>3</sup>; NAKANO, Toshihiko<sup>4</sup>; TAKAHASHI, Yukihiro<sup>5</sup>; IMAI, Masataka<sup>5</sup>; GOUDA, Yuya<sup>5</sup>; YOSIDA, Kazuya<sup>6</sup>; SAKAMOTO, Yuji<sup>6</sup>

<sup>1</sup>Graduate School of Science, Rikkyo University, <sup>2</sup>Department of Science, Rikkyo University, <sup>3</sup>Graduate School of Engineering, Osaka University, <sup>4</sup>Mechanical Engineering, Oita National College of Technology, <sup>5</sup>Graduate School of Science, Hokkaido University, <sup>6</sup>Graduate School of Engineering, Tohoku University

The planets have been optically observed by spacecraft and ground-based and space telescopes, which have provided many information on their atmospheres and plasmaspheres. It is important to conduct long-term continuous observations for studies on time-dependent events therein. Observations by spacecraft have an advantage that it is able to observe planets intensively with high spatial resolution during a rather short period (several years), however the observation geometry is not constant as the spacecraft orbits around the planet. Moreover, it is difficult to detect a fluctuation with time scales close to an orbiting period or a decade using an orbiter. On the other hand, remote sensing from the Earth can monitor a planet from a fixed direction for a long time in succession. A ground-based observation may accomplish high spatial resolution by using a telescope with a large diameter, though it is usually limited by seeing. A period of planetary observation from an observatory in the middle and low latitudes is not as long as 10 hours. Three observatories are required at least to continuously monitor a planet. Thus, observations of planets by spacecraft and ground-based telescopes are complimentary.

Then, we have been promoting the FUJIN-project, which aims at continuous observations of planets using a telescope lifted by a balloon in the polar stratosphere. FUJIN-2 will be launched at ESRANGE in Kiruna, Sweden in the window from May to July in 2016. The gondola will be recovered in Scandinavia after a circumpolar flight for two or three weeks. Although the primary study subject of the FUJIN-2 was Venus, we changed Venus to Jupiter. Because the diameter and aspect ratio of Venusian disk changes as its phases, a study subject of Venusian atmosphere depends on its phase. However, a chance of observation is quite limited. A launch window of a balloon cannot be freely selected. A circumpolar flight can be performed only during the summer season from May to July. So we concluded that Venus is not a suitable target of FUJIN. But, Jupiter can be observed under an almost same condition throughout the year except for the period of superior conjunction. We will observe Jupiter at the deepest absorbing band, methane (~890nm), in the visible to near-infrared region, and obtain a phase velocity and a wave number of planetary-scale waves and background wind velocity at a bright haze area near the polar region. Using these data, we will deduce parameters which are essential to identify the wave structure as the Rossby wave. Also, we will detect the cumulonimbus cloud in Jupiter and compare the positions of the clouds and the zones and the belts in the Jovian atmosphere, and study dynamics in the cumulonimbus cloud in Jupiter.

A simulation of the electric power in the polar orbit was performed. During daytime SCPs (Solar Cell Panels) of which the nominal maximum power is 540 W generates electric power for FUJIN-2, and during nighttime Li-ion batteries supply electric power. Under the condition of a circumpolar flight of FUJIN-2 from July 1 to 14 in 2016, we estimate that the SCPs can supply power larger than 330 W in average. Considering power required for charging the Li-ion battery the electric power which the system can consume is about 330 W and 191 W during daytime and nighttime, respectively.

Apart from that the control system of gondola (CMGs and DCP), a drive circuit of motors, an interface of CCD, a hood and its rotation system, and an extension of an airtight chamber of electric system are under development. Optical alignment of the telescope will be adjusted, and the image quality will be tested. After all of the sub-systems are integrated, a thermal vacuum test under the stratospheric environment will be conducted in fall in 2015. According to the test result the electric power required for the heaters will be determined. The functional tests will be completed by the end of 2015, and the FUJIN-2 gondola will be shipped to ESRANGE.

Keywords: FUJIN project, Jupiter, the polar stratosphere, continuous observations, balloon, FUJIN-2

## Mesospheric wind/temperature measurements in the terrestrial planetary atmosphere using the IR heterodyne spectroscopy

TAKAMI, Kosuke<sup>1\*</sup> ; NAKAGAWA, Hiromu<sup>1</sup> ; SAGAWA, Hideo<sup>2</sup> ; AOKI, Shohei<sup>3</sup> ; KASABA, Yasumasa<sup>1</sup> ; MURATA, Isao<sup>1</sup>

<sup>1</sup>Tohoku University, <sup>2</sup>Kyoto Sangyo University, <sup>3</sup>Istituto Nazionale di AstroFisica

The terrestrial planetary mesosphere is the transition region between thick lower atmosphere and thin upper atmosphere. The change of momentum between the surface and the mesosphere which occurs through breaking gravity waves perturbs wind and temperatures in the mesosphere, and potentially affects on atmospheric escape. Therefore, mesosphere provides us important information to understand atmospheric coupling between lower and upper atmosphere. However, there are still unsolved problems in the terrestrial planetary mesosphere due to the lack of observations. On Mars, the unexpected large amount of heavy ions ( $\text{CO}_2^+$ ,  $\text{O}_2^+$ ) was observed in the upper atmosphere [Carlsson et al., 2006]. The mechanism to propagate such heavy ions from lower atmosphere to upper atmosphere is necessary. On Venus, the characteristics of the transition region between retrograde zonal superrotation in the cloud layer and subsolar-to-antisolar flow in the upper atmosphere are not yet solved. Previous studies pointed out that the atmospheric waves have an important role on the transportation of momentum, energy and materials. The detailed measurement of atmospheric waves is required.

Ultra-high resolution heterodyne spectroscopy of  $\text{CO}_2$  at mid-IR wavelengths is one of the powerful tools to study wind and temperatures in the terrestrial atmospheres. Kinetic temperature can be calculated from the width of the observed lines and the doppler shift due to the wind is estimated from the difference between the measured line frequency and the  $\text{CO}_2$  rest frequency. In contrast to existing sub-mm observations, IR heterodyne spectroscopy offers a much higher spatial resolution allowing detailed study of temperature variations with latitude and local time. The IR heterodyne spectroscopy can achieve the spectral resolution  $\sim 10^7$  and high spatial resolution of 3.5 arcsec with 60cm telescope at  $10\mu\text{m}$ .

The purpose of this study is to investigate the methods to derive wind and temperature and its error estimation on Venus. Observations were carried out using Tuneable Heterodyne Infrared Spectrometer (THIS). The data was obtained in the east limb 33S on Venus in 4th June 2009 at the McMath- Pierce Solar Telescope of the National Solar Observatory on Kitt Peak in Arizona. Integration time is about 20 minutes. Because the exact altitude of the emitting region is predicted by the model to be  $\sim 110\text{km}$  with a half width of 10km, we can directly derived the wind and temperature in its altitudinal region. Our results indicated that the accuracies of derived wind and temperature were  $\pm 11\text{m/s}$  and  $\pm 12\text{K}$  respectively. These errors were defined from  $\chi^2 \leq 1$  of Gaussian fitting of the emission line. The estimated errors are sufficient to discuss disturbance of temperature on Mars and Venus (Mars:5-35K, Venus:5-40K [Deming and Mumma, 1983]). The estimated error of the wind basically agreed with the expected values from the spectral resolution ( $\pm 10\text{m/s}$ ). The obtained mesospheric temperature  $184 \pm 12\text{K}$  shows a good agreement with the in-situ measurement by Pioneer Venus [Clancy et al., 2008].

We developed the new IR heterodyne instrument for the dedicated telescope at the top of Mt. Haleakala, Hawaii. Using the methodology shown here, we plan to perform the continuous monitoring of wind and temperature in the Venus/Mars mesosphere.

Keywords: mesosphere, infrared, heterodyne, error, Mars, Venus

## Jovian tropospheric aerosols inferred from the Cassini ISS limb-darkening data

SATO, Takao M.<sup>1\*</sup> ; SATOH, Takehiko<sup>2</sup> ; ENOMOTO, Takayuki<sup>3</sup> ; KASABA, Yasumasa<sup>4</sup>

<sup>1</sup>Institute of Space and Astronautical Science, Japan Aerospace Exploration Agency, <sup>2</sup>Institute of Space and Astronautical Science, Japan Aerospace Exploration Agency, <sup>3</sup>The Graduate University for Advanced Studies, <sup>4</sup>Tohoku University

To obtain new observational constraints on the single scattering phase functions of aerosols in the Jovian upper troposphere, we have analyzed Cassini Imaging Science Subsystem (ISS) imaging data obtained at a wide range of solar phase angles (0-140 degrees) in two spectral channels (BL1: 455 nm, CB2: 750 nm) for a bright zone (STrZ) and a dark belt (SEBn). In this study, we applied the Mie theory for spherical particles to the tropospheric aerosols for simplicity. We found that the real refractive index ( $n_r$ ) of aerosols is much higher ( $n_r = 1.85$ ) than previous experimental values of  $n_r$  for  $\text{NH}_3$  ice particles. This would strongly suggest the idea that aerosols in the upper troposphere are not composed of pure  $\text{NH}_3$  ice.

Jovian tropospheric aerosols have been expected to consist of nonspherical particles from the atmospheric temperature in the upper troposphere. Application of Mie scattering theory to the tropospheric aerosols in Jupiter is a controversial issue when deducing the scattering properties from remote sensing data. We investigate how much robustness there is in the results obtained from our latest study, by comparing the best-fit Mie scattering phase functions derived from the Cassini ISS limb-darkening data with those for various nonspherical particles. Assuming that shape of nonspherical particles in the upper troposphere is spheroidal, we calculate the scattering phase functions for a wide variety of real refractive index, effective radius, and ratio of long axis to short axis. T-matrix method is used for this calculation. The scattering phase functions for spheroidal particles which have a near value ( $n_r = 1.45$ ) of real refractive index for  $\text{NH}_3$ -ice ( $n_r = 1.42$ ) are found to have weaker backward scattering compared with our best-fit Mie scattering phase functions. It is obvious that these scattering phase functions cannot reproduce the observed limb-darkening data. Conversely, several scattering phase functions for spheroidal particles ( $n_r = 1.85$ ) have similarity to our best-fit Mie scattering phase functions with respect to the strength and shape of scattering phase function. Based on this preliminary investigation, we can say that Jovian tropospheric aerosols are not composed of pure  $\text{NH}_3$ -ice particles even though we focus on the nonsphericity of these aerosols.

In this presentation, we will show the simulated limb-darkening curves calculated with the scattering phase functions for nonspherical particles, along with the observed limb-darkening curves.

Keywords: Jupiter, cloud structure, radiative transfer, Cassini

## Infrared imaging-polarimetric observations of Venus with NIIHAMA and SOLAR-C on Haleakala

ENOMOTO, Takayuki<sup>1\*</sup> ; SATOH, Takehiko<sup>2</sup> ; YONEDA, Mizuki<sup>3</sup> ; KUHN, Jeff<sup>4</sup>

<sup>1</sup>SOKENDAI (The Graduate University for Advanced Studies), <sup>2</sup>Institute of Space and Astronautical Science, Japan Aerospace Exploration Agency, <sup>3</sup>Planetary Plasma and Atmospheric Research Center, Graduate School of Science, Tohoku University, <sup>4</sup>Institute for Astronomy, University of Hawaii

To best utilize the polarization data from Venus, as a useful tool to study its atmosphere and aerosols, one needs to cover enough either a range of phase angles or spectra by observations. While most of previous studies were based on "phase curves" in a few visible wavelengths, we are motivated to perform multi-wavelength polarimetry in the infrared at a few selected phase angles. To acquire infrared imaging-polarimetric data of Venus, preparative works were done at the Institute for Astronomy (IfA), University of Hawaii, Maui.

From recent our visible-wavelength observations (2012 - 2014) using HOPS (Hida Optical Polarimetry System), we found that the optical thickness of polar hazes of Venus are now in thinning phase. Since polarization is dominated by the main cloud, it is difficult to significantly derive the optical thickness of decreasing hazes without affected by the errors due to an assumption that main cloud parameters are same as Hansen and Hovenier (1974). Additionally because the previous observations take long time to obtain polarization data varying with phase angle changes of Venus, it is a problem that variation of polarization can contain its temporal variations.

Considering the polarization of the infrared light scattered by H<sub>2</sub>SO<sub>4</sub> droplets with radius of 1.05 microns, standard Venusian cloud model (Esposito, 1980), the sign of polarization shall vary from negative to positive at middle phase angle range, between 60 and 80 deg. At this phase angle range, polarization degrees caused by single scattering vary like J: negative, H: neutral, K: positive (astronomical bands, central wavelength (microns) J: 1.25, H: 1.65, K: 2.2). Actually according to test calculations taking into account multiple scattering, disk-averaged polarization degree at phase angle 80 deg. J: -3%, H: -0.5% K: +2% are expected. In case that observed signs of polarization are different from that of expected, parameters such as radius of cloud particle can be different from standard cloud model. For example if main cloud particles are larger (~ 1.5 microns), these signs can vary like J: negative, H: negative, K: neutral. Inversely if the particles are smaller (~ 0.6 microns) J: neutral, H: positive, K: positive. From combination of these signs, we can know microphysical properties of the clouds with single observation run. Because especially phase angle around 80 deg. is near greatest elongation, which means that observation is much easier compared with other phase angles, we are planing to perform observations at that time.

To realize our idea, preparative works, optical design of SOLAR-C telescope with a polarizer (Savart plate) inserted into the optical system and test observations, were done from September through December 2014, and in February 2015 at IfA. The test observations were carried out by using NIIHAMA camera attached to SOLAR-C, off-axis gregorian telescope of diameter 45cm, at the top of Haleakala altitude about 3000m. The Savart plate separates the light into two beams whose vibrating plane is orthogonal each other. We could verify that the separation distance is about 200 pixels on images (pixel scale ~ 0.45 arcsec./pixel) by the observations. For precise measurements of polarization degrees, calibration of polarization generated by primary mirror of SOLAR-C is future work.

Keywords: Venus, Aerosols, Imaging-Polarimetry

## 5um spectro-imaging on the Venus dayside

KANO, Sakimi<sup>1\*</sup> ; IWAGAMI, Naomoto<sup>1</sup> ; HOSOUCI, Mayu<sup>1</sup> ; SUZUKI, Fumiharu<sup>1</sup>

<sup>1</sup>Department of Earth and Planetary Science, Graduate School of Science, The University of Tokyo

In the Venus atmosphere, the wind speed increases with height and reaches about 100 m/s at the cloud top, which corresponds to an angular velocity 60 times faster than the rotation of the planet. It is called super-rotation and its generation mechanism is unknown. To investigate atmospheric wave structures in the cloud region (50-70km), which is said to be important as the acceleration region, most studies have used the ultraviolet wavelength to image atmospheric waves at 70 km. Some studies have used the infrared wavelength and analyzed thermal emissions from the nightside to image atmospheric waves at 50 km. We performed infrared spectroscopic measurements using IRTF/CSHELL in May 2014. Our observation aimed at imaging the waves at 60 km and another altitude region simultaneously. We obtained the distributions of cloud height deviation at 60 km by quantifying carbon dioxide absorption in the 1.07um wavelength region. The distributions of cloud temperature at 70 km were also obtained from 5.04um wavelength region. In this presentation, we will show the latter results and discuss the wave structure at 70 km.

Keywords: Venus, super-rotation

## Implementation of sulfuric acid cloud into a Venus GCM

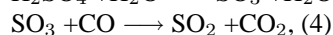
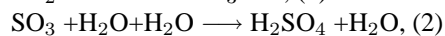
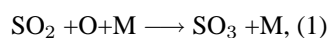
ITO, Kazunari<sup>1\*</sup>; KURODA, Takeshi<sup>1</sup>; KASABA, Yasumasa<sup>1</sup>; TERADA, Naoki<sup>1</sup>; IKEDA, Kohei<sup>2</sup>; TAKAHASHI, Masaaki<sup>3</sup>

<sup>1</sup>Graduate School of Science, Tohoku University, <sup>2</sup>National Institute for Environmental Studies, <sup>3</sup>Atmosphere and Ocean Research Institute, University of Tokyo

Venus has global sulfuric acid (H<sub>2</sub>SO<sub>4</sub>) cloud deck in the altitude of 50-70 km. Past reproductions of cloud distributions in numerical models have been tried using VGCMs (Venusian General Circulation Models) with cloud parameterization (condensation / evaporation and sedimentation processes) in Lee et al. [2010] and our group (e.g. Kato et al. [2014]). However, they did not include chemical processes, and did not reproduce the cloud cycle based on realistic processes.

We have tried to implement the chemical processes related to H<sub>2</sub>SO<sub>4</sub> clouds into our VGCM and to reproduce the realistic production and extinction of clouds. As Kato et al. [2014], we used a VGCM based on the CCSR/NIES/FRCGC AGCM [Ikeda, 2011]. Horizontal resolution is T21 (longitude and latitude grid : about 5.6 degree). In vertical, the model has 52 levels (the top altitude: about 95 km). For cloud condensation/evaporation processes, we assumed that if the mixing ratio of H<sub>2</sub>SO<sub>4</sub> (sum of vapor and cloud) is larger than the calculated saturated level, i.e., the supersaturated H<sub>2</sub>SO<sub>4</sub> concentrates as an aerosol, and if not the H<sub>2</sub>SO<sub>4</sub> aerosol all evaporates. The radius of cloud aerosol is distributed into 4 modes by ratios based on Haus and Arnold[2010]. It means that our model at the moment does not include the growth of particle size, and only traces the advection of produced clouds. We also note that the produced cloud distributions should modulate the thermal distributions through radiative effects but current our model assumes constant heat input profile (as well as the former code).

In this study, we implement following chemical reactions (1) – (4) into the VGCM.



After 15 Venus days, the cloud distribution in this model reaches equilibrium status. In this model, we succeeded to reproduce the cloud cycle, i.e., the formation of H<sub>2</sub>SO<sub>4</sub> cloud particles in the upper cloud region (about 67-75 km altitude) and the formation of SO<sub>2</sub> and its extinction in the lower cloud region (about 50km altitude). This is consistent with the formation / extinction processes suggested by a two-dimensional model [Imamura and Hashimoto, 1998]. This model could also qualitatively reproduce the cloud top altitude with latitude. However, optical thickness in polar region (more than 75 degree) was smaller than Venus Express observations [Haus et al., 2014]. Another problem is that the mixing ratios of H<sub>2</sub>O and SO<sub>2</sub> were larger than those in a chemical model [Krasnopolsky, 2012]. We are now trying to solve these problems.

As the next step, we will implement the radiative effects of H<sub>2</sub>SO<sub>4</sub> clouds into the VGCM, and enable to produce more realistic thermal structure. We will apply this model for studying qualitatively and quantitatively clouds global distributions and their variation which will be observed by Akatsuki mission from 2016.

Keywords: Venus, sulfuric acid cloud, General Circulation Model



## Study about the structure of Venusian lower atmosphere

ANDO, Hiroki<sup>1\*</sup> ; IMAMURA, Takeshi<sup>1</sup> ; TAKAGI, Masahiro<sup>2</sup>

<sup>1</sup>ISAS/JAXA, <sup>2</sup>Kyoto Sangyo University

Venus is enveloped by a thick cloud, which is composed of sulfuric acid and located at the altitude of 50-70 km. The atmospheric structure above the cloud layer has been observed by optical measurements in Pioneer Venus and Venus Express missions. However, the thick cloud prevents us investigating the atmosphere below the cloud layer. There are few observations to examine the temperature and wind speed by probes, but probe measurements can observe only the specific place. One of the most useful methods to investigate the atmospheric structure below the cloud layer is radio occultation measurement, which can retrieve the vertical temperature profile with high precision (vertical resolution ~1 km and temperature measurement error ~1 K). In this study we analyzed the radio occultation data obtained in Venus Express mission and retrieved vertical temperature profile globally.

The analysis period of data is 2006 to 2010, and the number of temperature profiles is 280. All the temperature profiles are classified at each latitude bin, which is divided every 10° degree, and averaged in the vertical direction with the width of 1 km. In this study the hemispheric and localtime dependences are not considered. As a result, there is a clear difference of the atmospheric structure between low and middle altitudes and high latitudes. In low and middle latitudes the neutral stable layer is located in the altitude of 50-60 km, and the atmosphere is weakly stable under 50 km altitude. In the high latitudes the neutral stable layer is consecutively located in the altitude of 40-60 km. In this presentation we will discuss what generates the difference of the atmospheric structure below the cloud layer by comparing with the numerical result obtained in a general circulation model named AFES.

Keywords: Venus atmosphere, Venus Express, Radio occultation, GCM

## Radio holographic analysis of Venus' radio occultation data

MIYAMOTO, Mayu<sup>1\*</sup>; IMAMURA, Takeshi<sup>2</sup>; ANDO, Hiroki<sup>2</sup>; TSUDA, Toshitaka<sup>3</sup>; AOYAMA, Yuichi<sup>4</sup>

<sup>1</sup>Department of Earth and Planetary Science, The University of Tokyo, <sup>2</sup>Japan Aerospace Exploration Agency, Institute of Space and Astronautical Science, <sup>3</sup>Research Institute for Sustainable Humanosphere, <sup>4</sup>National Institute of Polar Research

Gravity waves are considered to drive the atmospheric general circulation by vertical transportation of momentum and energy. Gravity wave breaking occurs via local instabilities such as convective instability and shear instability as the amplitude of the wave increases in the course of upward propagation. Turbulence following the gravity wave braking plays an important role in the diffusion of atmospheric substances, momentum, and energy.

Gravity waves with vertical wavelengths from a few tens of meters to kilometers have been observed in the Earth's atmosphere by radiosondes and radars. Also in the atmospheres of other planets, gravity waves are observed by various methods including radio occultation. The radio occultation method relies on the measurement of the frequency shift of the received signal caused by the bending of radio waves in the radial gradient of the refractive index in the atmosphere.

The geometrical optics method has long been used for the analysis of radio occultation data. However, this method cannot disentangle multipath rays and vertical resolution is limited by the size of the Fresnel zone (~1 km). Because of this limitation, only a limited part of the gravity wave spectrum has been covered, and thus the propagation and dissipation mechanisms of the gravity waves in other planets are poorly understood.

Radio holographic methods have been proposed for processing of radio occultation signals in multipath regions and obtaining atmospheric profiles with high resolution. One of them is the Full Spectrum Inversion (FSI), which was recently applied to GPS occultation data of the Earth's atmosphere. By applying this technique to Venus Express radio occultation data, we derived temperature profiles with high vertical resolution. In this presentation, the vertical wave number spectra will be compared among different altitudes, latitudes, and longitudes, and the spatial distribution of unstable layers will be investigated for studying propagation and dissipation of the gravity waves.

Keywords: Venus, Gravity wave, Radio occultation, Radio holographic analysis

## Effect of the terrestrial ionosphere for the lunar radio occultation observation

KIKUCHI, Fuyuhiko<sup>1\*</sup> ; KAWANO, Nobuyuki<sup>2</sup> ; MATSUMOTO, Koji<sup>1</sup>

<sup>1</sup>RISE project office, National Astronomical Observatory of Japan, <sup>2</sup>National Astronomical Observatory of Japan

The existence of the lunar ionosphere is an open question of the Moon. The lunar ionosphere was found by radio occultation observations of spacecraft, such as Luna 19, Luna 20, and SELENE (Vasilyev et al., 1974; Vyshlov et al., 1976; Imamura et al., 2012). However, the estimated electron densities of several hundreds to 1000 cm<sup>-3</sup> are much larger than theoretical estimation (Daily et al., 1977). Although several kinds of theories have been proposed to explain the existence of the lunar ionosphere (Daily et al., 1977, Savich 1976, Stubbs et al., 2011), inadequate quality and quantity of the present data prevent to qualify the origin of the lunar ionosphere.

Principal factor of inadequate data is the terrestrial ionosphere. The amplitude for fluctuation of total electron content (TEC) of the terrestrial ionosphere is similar or larger than the TEC of the lunar ionosphere. The cause of the lunar ionosphere cannot be derived without removal of the terrestrial ionosphere.

Imamura et al. (2012) removed the terrestrial ionosphere by a polynomial fitting method. If we assume the lunar ionosphere exists under a certain altitude (for example 30 km), the time series of observed TEC can be divided to two parts depending on whether the radio signal paths the lunar ionosphere or not. Before the occultation starts, named A-part, only the terrestrial component of the TEC is included in the observed TEC. On the other hand, both of the terrestrial and lunar components are included in the occultation period, named B-part. To remove the terrestrial component of B-part, the observed TEC of A-part is fitted by polynomial function and extrapolated to B-part. The lunar TEC had been estimated by this method in SELENE mission. However, the polynomial approach was ineffective when the fluctuation of the terrestrial ionosphere was large (Imamura et al., 2012).

In this presentation, the effect of the terrestrial ionosphere for the radio occultation observation is estimated by using SELENE-derived terrestrial TEC data. The error of the polynomial fitting and extrapolation of above method is evaluated, and the possibility of the detection of the lunar ionosphere is discussed. The optimal configuration of the radio occultation observation is also considered for future exploration. Appropriate orbital elements are discussed to collect sufficient data set. We focus on a solar zenith angle dependency of observation that is a key parameter to derive a mechanism for generating the lunar ionosphere. Furthermore, we start to search the lunar ionosphere by using other data set of SELENE. That is the VLBI data obtained in VRAD mission. Both of S-band and X-band signals from sub satellite of SELENE, Vstar, were received at four ground stations of VERA. The result will be shown in the presentation.

[1] Vasilyev, M. B. et al., Radio transparency of circumlunar space using the Luna-19 station, *Cosmic Res.*, 12, 102-107, 1974.

[2] Vyshlov, A. S. et al., Some results of cislunar plasma research, *Solar-Wind Interaction with the Planets Mercury, Venus, and Mars*, NASA, 81-85, 1976.

[3] Imamura, T. et al., Radio occultation measurement of the electron density near the lunar surface using a subsatellite on the SELENE mission, *J. Geophys. Res.* 117, 2012.

[4] Daily, W. D. et al., Ionosphere and atmosphere of the moon in the geomagnetic tail, *J. Geophys. Res.*, 82, 5441-5451, 1977.

[5] Savich, N. A., Cislunar plasma model, *Space Res.*, 16, 941-943, 1977.

[6] Stubbs, T. J. et al., A dynamics fountain model for lunar dust, *Adv. Space Res.*, 37, 59-66, 2006.

Keywords: Moon, ionosphere, radio occultation

## The Terrestrial Exosphere observed by Space Satellites

KUWABARA, Masaki<sup>1\*</sup>; YOSHIOKA, Kazuo<sup>2</sup>; MURAKAMI, Go<sup>2</sup>; TSUCHIYA, Fuminori<sup>3</sup>; KIMURA, Tomoki<sup>2</sup>; KAMEDA, Shingo<sup>4</sup>; SATO, Masaki<sup>4</sup>; YOSHIKAWA, Ichiro<sup>1</sup>

<sup>1</sup>Univ. of Tokyo, <sup>2</sup>ISAS/JAXA, <sup>3</sup>Tohoku Univ., <sup>4</sup>Rikkyo Univ.

The terrestrial exosphere is the outmost region of the atmosphere, where scale height of particles is longer than the mean free pass of them. Thus exospheric particles are collisionless each other. Hydrogen atoms are most abundance in the terrestrial exosphere and helium atoms are the secondary components. These atoms resonantly scatter sunlight and build the ultraviolet glows surrounding the Earth, called "geocorona".

In 1972, Apollo 16 obtained the first image of the geocorona from the lunar orbit with approximately field-of-view of 10  $R_E$ . In 1988, furthermore, the Ultraviolet Imaging Spectrometer (UVS) onboard the Nozomi satellite gave us the geocorona expanding down to 20  $R_E$ . Therefore the observation of Apollo-16 was not enough to image whole geocorona. No observations of the geocorona had been done so far.

The observations of the geocorona have also been conducted by the Earth-orbiting satellites. Recently, hydrogen atoms in the geocorona surrounding from 3  $R_E$  to 8  $R_E$  are reported to increase by approximately 10% during magnetic storms. However, the responsible mechanism has not been proposed.

In September 2013, HISAKI/EXCEED was launched by the Epsilon rocket. It is now observing the geocorona in the orbit. During the strong geomagnetic storms in February 2014, the brightness at the Lyman-alpha emission was identified. I found the responsible mechanism to increase the brightness during the magnetic storms and compared it with observations. As a result, I have made a conclusion that thermospheric expansion and charge exchange with plasmaspheric ions should be responsible for the increases of hydrogen atoms.

In December 2014, the ultra-small deep space satellite (PROCYON) launched together with HAYABUSA-2. Lyman Alpha Imaging Camera (LAICA) is boarded on PROCYON. The LAICA instrument observes the solar resonant scattering lights from hydrogen atoms. It takes pictures of whole geocorona with a wide FOV (corresponding to more than 25  $R_E$  from Earth). I have calibrated the performance of the LAICA before the launch. As a result, the LAICA has a total sensitivity of  $1.1 \times 10^{-3}$  cps/Rayleigh/pix at H I (121.6nm). Then, on 5th January 2015, I succeeded in imaging the geocorona from the deep space (13,000,000 km away from Earth). Not only it was 42 years after the Apollo-16 observation, but also this geocoronal imagery has the widest perspective in the world.

Keywords: exosphere, plasmasphere, magnetosphere, magnetic storm, geocorona, lyman alpha

## A global MHD simulation study of the ion outflow channels from the Martian ionosphere

MAEDA, Sawa<sup>1\*</sup> ; TERADA, Naoki<sup>1</sup> ; KASABA, Yasumasa<sup>1</sup>

<sup>1</sup>Graduate School of Science, Tohoku University

Mars has no global magnetic field, leading to the direct interaction of the solar wind with its upper atmosphere. As a result of the direct interaction escape of planetary atmosphere occurs. In the past, the Phobos2 spacecraft observed the acceleration and outflow of ions of planetary origin, and the oxygen loss rate from present-day Mars was estimated about  $3 \times 10^{25}$  ions/s [Lundin et al., 1989]. Also, Ion Mass Analyzer (IMA) aboard Mars Express (MEX) observed a large amount of heavy ions such as  $\text{CO}_2^+$  escaping from the Martian ionosphere [Carlsson et al., 2006].

A variety of outflow processes that result from the direct interaction of the solar wind have been proposed, such as the ion pick-up process, sputtering, outflow from magnetic anomalies, and outflow of the ionospheric ions. Among them, the outflow process of low energy ions ( $< \sim 10\text{eV}$ ) from the ionosphere is especially uncertain because observations are technically difficult. Therefore, we performed a three-dimensional visualization using the result of a global magnetohydrodynamics (MHD) simulation of the Mars-solar wind interaction [e.g., Terada et al., 2009], and analyzed the outflow channels and acceleration mechanisms of the low energy ionospheric ions. The MHD simulation treats plasma as a fluid, and we used it because the fluid approximation relatively holds for the low energy ions due to their small Larmor radii. As results of a three-dimensional visualization, we found that a streamline extending from the dayside ionosphere goes through near a magnetic pole of Mars, and splits into east and west in the vicinity of the equatorial plane in the night side ionosphere and coils up. It eventually forms four vortices. Bulk velocity along these vortices increase near the ionopause, extending to outer space. In this study, at first, we followed the streamlines and examined where the ions originating from the dayside ionosphere were accelerated. Then, we chose some streamlines, checked the values of the bulk velocity, the magnetic field, and the plasma pressure along them, and quantitatively evaluated all the terms of the equation of motion. Thereby, we examined where and by what force the ions of the dayside ionospheric origin were accelerated over the chosen streamlines.

In this presentation, we will present the results of the analysis of the outflow channels and the acceleration mechanisms of the ionospheric ions at Mars using the global MHD simulation.

Keywords: Mars, ionosphere, atmospheric outflow, MHD simulation

## A simulation study of the Kelvin-Helmholtz instability at the Martian ionopause

AIZAWA, Sae<sup>1\*</sup> ; TERADA, Naoki<sup>1</sup> ; KASABA, Yasumasa<sup>1</sup>

<sup>1</sup>Dep. Geophysics, Graduate School of Science, Tohoku Univ.

Because the Mars has no intrinsic magnetic field, the solar wind flow directly interacts with the planetary ionosphere. Under the circumstances, planetary ionopause is a density discontinuity surface and a velocity shear surface between the magnetized solar wind flow and the planetary ionosphere. The ionopause is subject to the Kelvin-Helmholtz (KH) instability [Amerstorfer et al., 2010], which is expected to play a role in removing ionospheric materials from the planet. In addition, the KH instability may cause a dawn-dusk asymmetry at the magnetopause because of the finite Larmor radius (FLR) effect of ions [Nagano, 1978]. At an ionopause, for the same reason, the KH instability may cause an asymmetry in the direction of the solar wind motional electric field.

Terada et al. [2002] pointed out that the KH instability at the Venusian ionopause develops asymmetrically through the acceleration of ionospheric ions in the direction of the solar wind motional electric field, using a global hybrid simulation. It is well known that the ion FLR effect, the gravitational stabilizing effect, the effect of the thickness of the boundary layer, etc. determine the initial growth of the KH instability. Unfortunately, it was difficult to separately evaluate each contribution of these effects with a global simulation. In addition, a study of the ion FLR effect with the parameters around the Martian ionopause is yet to be done.

In this study, we will estimate the escape rate of the Martian atmosphere by the KH instability considering the ion FLR effect and the gravitational stabilizing effect. We will investigate contribution of each effect to the linear growth rate and non-linear evolution of the KH instability in a parameter range around the Martian ionopause. As a first step of this study, we compare an ideal MHD simulation to an MHD simulation including the FLR effect to investigate its effect on the linear growth rate and non-linear evolution of the KH instability. In this presentation, initial results obtained by these numerical simulations will be presented.

Keywords: the Kelvin-Helmholtz instability, the finite Larmor radius effect